Thermal Ammonolysis Study o fthe Rare-Earth Tantalates RTaO4

Pascal Maillard, Franck Tessier, Emmanuelle Orhan, François Cheviré, Roger Marchand

Thermal Ammonolysis Study of the Rare-Earth Tantalates $RTaO_4$

Pascal Maillard, Franck Tessier*, Emmanuelle Orhan, François Cheviré and Roger Marchand

UMR CNRS 6512 "Verres et Céramiques", Institut de Chimie de Rennes, Université de Rennes 1, 35042 Rennes Cedex, France

* To whom correspondence should be addressed: Franck.Tessier@univ-rennes1.fr

Reaction between rare-earth tantalates $RTaO_4$ and ammonia flow at 900-950°C forms oxynitrides belonging to different structure types, perovskites $RTaON_2$, pyrochlores $R_2Ta_2O_5N_2$ and defect fluorites $RTa(O,N,\square)_4$, depending on the size of the R element. The nature of the oxide precursor is a crucial parameter affecting the ammonolysis reaction. A comparative study has been carried out between oxide powders prepared by a ceramic route and a *chimie douce* process. The pyrochlore structure is restricted to large rare-earths (R=Nd→Gd). For smaller R elements, thermal ammonolysis of reactive precursors elaborated from the citrate combustion route results in a fluorite-type oxynitride solid solution. X-ray and neutron diffraction studies evidence a totally disordered cubic fluorite unit cell, which, however, appears to be not suitable for the structure refinement, thus revealing a more complex atom arrangement.

Introduction

Oxides are not only useful precursors for the synthesis of oxynitrides, they constitute also an excellent basis of comparison for their characterization which may be considered as the study of modifications brought by the nitrogen/oxygen substitution. Attractive properties directly related to the role played by nitrogen can result from this N/O substitution [1-3].

The behavior of the rare-earth tantalates $RTaO_4$ (R = La→Yb, Y) heated in flowing ammonia at 900-950°C has been investigated previously as leading to perovskite and/or pyrochlore oxynitrides depending on the size of the rare-earth [4]. In particular, Pors *et al.* have described formation of $R_2Ta_2O_5N_2$ pyrochlores for R = Nd→Yb and Y, the stability of which increases for smaller elements so that single phases could be isolated from R = Er.

In the present work, as part of a continuing study of rare-earth and transition metal oxynitrides exploring in particular *chimie douce* approaches, we have revisited the crystal chemistry of the R-Ta-O-N oxynitrides. While the stoichiometry $R_2Ta_2O_5N_2$ and the pyrochlore structure were confirmed for the larger rare-earths (R = Nd→Gd), we have evidenced, using X-ray and neutron diffraction, a different structure-type for the smaller rare-earths which give rise, actually, to fluorite-type phases, as illustrated here with R = Ho, Er, Yb and Y.

A particular interest was devoted to elaborate reactive precursors by involving complexation-calcination methods, typically the amorphous citrate route. Among several advantages, this method can induce formation of metastable phases, for example the cubic polymorph of the rare-earth tungstates R_6WO_{12}, which normal synthesis requires temperatures over 1200°C [5]. However, its essential interest lies in an improved reactivity towards ammonolysis which makes possible a decrease in the nitridation temperature onset and, consequently, an extension of the oxynitride thermal stability domain.

The R-Ta-O-N oxynitrides with fluorite structure we have isolated form solid solution domains with variable nitrogen content and powder color. Previous results obtained from rare-earth tungstates have shown interest of such composition domains for colored pigments applications, where it is possible to modify the powder color and hold it to a well-defined shade by only adjusting the nitrogen enrichment [3,6].

Furthermore, it should be noted that, in addition to luminescence properties [7,8], the rare-earth tantalates $RTaO_4$ show photocatalytic activity for water splitting [9]. Corresponding colored oxynitride compositions are potentially of interest for visible-light-driven photocatalysts, as already observed for tantalum oxynitrides [10-12].

Experimental

Preparation of oxide precursors. $RTaO_4$ tantalates were prepared both by a conventional ceramic route and by taking advantage of a *chimie douce* process - the amorphous citrate route – which gives the oxide precursors an enhanced homogeneity and reactivity towards ammonolysis.

Solid state route. The starting ternary oxides $RTaO_4$ were prepared by heating at 1400°C, in a muffle furnace, appropriate mixtures of rare-earth oxide and Ta_2O_5. Three cycles of 12 hours heating with intermediate grinding were often necessary to obtain X-ray pure phases.

*Amorphous citrate route***.** Among numerous *chimie douce*-type processes which have been developed to prepare oxide powders in order to improve their quality (purity, chemical homogeneity, etc.) and their reactivity, the process involving citric acid as a complexing agent was preferentially used. It is not, strictly speaking, a classic sol-gel process in the usual sense that the gel is not formed by a metal-oxygen-metal network, but rather from calcination of metal-organic complexes, thus producing ultrafine reactive powders with an excellent chemical homogeneity [3]. Rare-earth oxides separately dissolved in concentrated hydrochloric

acid (37 %, Merck) and a tantalum oxalate solution (H.C. Starck, [Ta_2O_5] = 175 g L^{-1}) were used as starting materials. Citric acid ($C_6H_8O_7$, ≥ 99 %, Merck) dissolved in a minimum amount of water was added to each solution in the proportion of one mole per cation valence, the addition being followed by a 20 min stirring step at 120°C. As the complexation of cations by citric acid is improved at pH ≥ 7, the acidic solutions were neutralized by ammonia solution (25 %, Merck) [13]. The solutions were then mixed and the resulting solution stirred at 150°C for 20 min to promote polymerization. The liquid was then progressively heated up to 250°C, leading after 5 h to an expanded black solid residue. This solid was finally ground and calcined at 600°C in air in an alumina crucible until total elimination of carbon.

Thermal ammonolysis. Nitridation reactions were carried out in alumina boats placed inside an electric furnace through which ammonia gas flowed with a flow rate of 40-50 L h^{-1}. The temperature was raised in the 900-950°C range at a heating rate of 10°C min^{-1}. Generally after 15 h reaction time, the furnace was switched off and the nitrided powders were allowed to cool to room temperature under pure nitrogen atmosphere.

X-ray diffraction. XRD powder patterns were recorded using a Philips PW3710 diffractometer operating with Cu K_α radiation (λ = 1.5418 Å). X'PERT softwares – Data Collector and Graphics, and Identify – were used, respectively, for pattern recording, analysis and phase matching. The lattice parameters were refined using Dicvol. [14]

Neutron diffraction. Neutron diffraction experiments were performed on the two-axis powder diffractometer 3T2 at the Orphée 14 MW reactor of the CEA Saclay (France), using λ = 1.2251 Å as the neutron wavelength. The diffraction pattern of the oxynitride powder was recorded over the angular range $6° < 2\theta < 120°$ in steps of 0.05°. The crystal structure of the oxynitride was refined using the Rietveld method with Fullprof [15].

Elemental analysis. Nitrogen and oxygen contents were determined with a LECO TC-436 analyzer using the inert gas fusion method. Nitrogen was measured as N_2 by thermal conductivity and oxygen as CO_2 by infrared detection. The apparatus was calibrated using N_2 and CO_2 gas (purity ≥ 99.95 %) as well as ε-TaN as a nitrogen standard [16].

Specific surface area. A Flowsorb II 2300 Micromeritics apparatus was used to determine the specific surface area of the powders by the single point BET method. Before measurement, the samples were outgassed under He/N_2 flow between 100 and 200°C for 30 min.

Results and Discussion

Two groups of rare-earth tantalates $RTaO_4$ can be distinguished from a crystallographic viewpoint, according to the rare-earth size. With R = La→Pr, they show a $BaMnF_4$-type structure and a $LaTaO_4$-type structure, both related to perovskite [17,18]. The tantalates containing smaller rare-earths (R = Nd→Lu, Y) are characterized by a fergusonite-type monoclinic unit cell at low temperature and a tetragonal one at high temperature, which form corresponds to a scheelite-type phase usually obtained through a reversible phase transition at temperatures higher than 1300°C [19].

As described previously [20], thermal ammonolysis of $LaTaO_4$ prepared by the ceramic route only results in a distorted perovskite-type oxynitride, $LaTaON_2$. Its crystal structure was refined recently by X-ray and neutron diffraction from a well-crystallized powdered sample resulting from a mineralisator-assisted ammonolysis [21]. It was solved in the C2/m space group (a = 8.0922(31) Å , b = 8.0603(2) Å, c = 5.7118(2) Å, β = 134.815(1)°), showing an ordered anionic sublattice. From R = Nd → Dy, Ho, thermal ammonolysis of the $RTaO_4$ fergusonites showed coexistence with the perovskite of another phase, less rich in nitrogen,

assumed to be a pyrochlore $R_2Ta_2O_5N_2$ [3,4]. Its stability increasing as the rare-earth ionic radius decreases, it could be obtained as a single phase with R = Er→Yb and Y. The corresponding cubic lattice parameters of the so-called "pyrochlores" are listed in Table 1, going from 10.56 Å for R = Nd to 10.235 Å for R = Yb [4]. $RTaON_2$ perovskites with R = Nd and Sm crystallize in an orthorhombic $GdFeO_3$-type unit cell [20]. We have shown in this study that $GdTaON_2$ presents the same deformation, unlike it was previously observed (cubic unit cell, a = 4.022(1) Å) [20]. Unit cell parameters have been refined to a = 5.552(3) Å , b = 5.690(2) Å and c = 7.923(3) Å (after XRD pattern in Fig. 1). The citrate route was also advantageously utilized to prepare the gadolinium oxynitride phase which was unambiguously identified as a pyrochlore (Fig. 2). Starting from an X-ray amorphous $GdTaO_4$ precursor calcined at 650°C, the reaction under ammonia flow at 900°C for only 5 h produced an orange powder with a refined cubic unit cell parameter a = 10.42(1) Å (Table 1). Its elemental analysis gave a nitrogen content (3.72 ± 0.06 wt.%) slightly higher than the calculated value (3.57 wt.%) for $Gd_2Ta_2O_5N_2$, indicating presumably beginning formation of the nitrogen-rich perovskite oxynitride $GdTaON_2$ (N wt.% = 7.33). The perovskite formation was confirmed for higher reaction times by the presence of extra weak peaks, as clearly observed in Fig. 2 after 15 h nitridation at 900°C.

In the case of smaller rare-earths Ho, Er, Yb and Y, we have studied the influence of the preparation method of the oxide precursors on the nature of the ammonolysis products.

$RTaO_4$ tantalates (R = Ho, Er, Yb and Y) prepared by the ceramic route were nitrided at 950°C. Under these conditions, the reaction kinetics is quite slow, requiring 5 nitridation cycles - 15 h each - to totally eliminate the starting oxide from the final product. Fig. 3a displays a representative X-ray powder pattern of that series obtained after ammonolysis of $HoTaO_4$. No single oxynitride was isolated due to the presence of extra peaks belonging to a perovskite phase. While we can confirm unambiguously the pyrochlore structure for the

larger rare-earths (for ex. Nd or Sm), X-ray powder patterns for smaller R elements (R = Ho→Yb, Y) are indexed in a fluorite-type unit cell with 1/8 the volume (space group $Fm\bar{3}m$). Comparison between Figures 2 and 3a shows that the pyrochlore-type X-ray powder pattern differs from a fluorite one by an additional low intensity peak (hkl: 311) located at 2θ ~28.8° (Cu K_α) which requires to double the fluorite cubic unit cell parameter. It could be thought logical *a priori* not to find that peak in the case of Ho, Er or Yb, as their atomic number (Z = 67, 68 and 70, respectively) is relatively close to that of tantalum (Z_{Ta} = 73), but in the case of Y (Z_Y = 39), this peak should be present if a cationic order existed, like in an $A_2B_2X_7$ pyrochlore-type arrangement. Actually, from dysprosium onwards, the oxynitride phase which forms is really a fluorite, not a pyrochlore. Several attempts were carried out at lower temperature (925°C) to only have the fluorite, but this temperature corresponds more or less to the reaction onset. On the other hand, an ammonolysis carried out at 1000°C induced a mixed-valent state of tantalum as indicated by the black color of the resulting powder. Mixtures were obtained also with the other R elements (R = Er, Yb and Y) studied, evidencing the limit of the ceramic route: the starting oxides are well crystallized powders with low specific surface area, and consequently low reactivity.

On the contrary, a complexation-calcination method could synthesize fine powders, potentially able to react with ammonia at lower temperature [22]. Illustrated by $HoTaO_4$, the citrate route yields a black expanded solid which gives after progressive calcination up to 600°C an X-ray amorphous diffraction powder pattern. Heatings performed at higher temperature, up to 900°C, improve the crystallization of the powder, without reaching, however, a better crystallization degree than that shown in Fig. 4, where a comparison is made with the diffraction profile of the same composition, $HoTaO_4$, prepared by a conventional route. Let us observe that the citrate route does not lead to the expected fergusonite, but to the high temperature scheelite polymorph. This phase being metastable, its

heating at higher temperature than ~900°C induces rapidly the phase transition scheelite → fergusonite, as the latter is thermodynamically stable up to ~1300°C. Scheelite phases $ErTaO_4$, $YbTaO_4$ and $YTaO_4$ were isolated in the same way at low temperature. As illustrated in Fig. 3b with holmium, these scheelite-type tantalates (R = Ho, Er, Yb and Y) can be nitrided as low as 900°C and transformed easily into pure fluorite oxynitride phases. Only one 15 h treatment in flowing ammonia was enough to prepare dark yellow oxynitride powders. The proportion of incorporated nitrogen increases as a function of nitridation temperature and time, thus delimiting in each case an oxynitride solid solution domain (Table 2). This progressive nitrogen enrichment is balanced by an increasing number of vacancies. As the electroneutrality rule requires that 3 O^{2-} are replaced by 2 N^{3-}, according to the following equation: 3 O^{2-} = 2 N^{3-} + 1 □, one vacancy is created per two introduced nitrogen atoms. It results in a slight decrease in the cubic unit cell parameter value. Let us note that after long nitridation times (> 90 h) at 900°C, extra weak peaks belonging to a perovskite-type oxynitride phase became detectable.

Another clear indication of the existence of continuous solution domains was the powder color after reaction, as the progressive nitrogen enrichment resulted in a continuous color variation related to the shift of the absorption edge position in the Visible [6]. If we choose the case of yttrium which does not show any interference with f-type transitions, the color of the $YTa(O,N,□)_4$ powders varies from yellow (after 15 h) to brown for the most substituted compositions (after 90 h).

Furthermore, we have observed that the synthesis of the fluorite oxynitrides was easier when starting from a scheelite precursor than from a fergusonite one. Two relevant arguments can be set out to explain the reaction kinetics, the morphology of the precursors and their crystal structure. On one hand, the reactivity of the "citrate route" powder is

correlated with a high specific surface area (≥ 15 $m^2 g^{-1}$), compared to a "ceramic route" powder (< 2 $m^2 g^{-1}$). The ammonolysis consists of a solid-gas reaction where the nitrogen species have to diffuse deep inside the grains of powder to produce an homogeneous nitrided phase, while corresponding oxygen is removed as water vapor. Consequently, high specific surface areas will lead more effectively to powders homogeneously nitrided to the core. On the other hand, from a structural viewpoint the fluorite structure looks closer to the scheelite structure which can be described as resulting from the stacking of two fluorite unit cells [23]. The change from fluorite to scheelite amounts to a cationic ordering and a global shift of the anions towards Ta atoms (in our case).

To sum up, we can state that cationic order (or the pyrochlore structure) exists for the large rare-earths when the disparity of ionic radius is really significant, while a disordered $RTa(O,N,\square)_4$ phase (or a defect fluorite structure) is formed with the smaller elements, from Ho, or even Dy. It is surprising, however, to index the XRD powder patterns in a small fluorite unit cell, which implies necessarily a single cationic position when the ionic radii (in eightfold coordination, after Shannon [24]) are rather different: Ta^{5+}: 0.74 Å; Dy^{3+}, $Ho^{3+} \rightarrow Yb^{3+}$: 1.027 Å, 1.015 Å→0.985 Å (Y^{3+}: 1.019 Å). Actually, a structure refinement by the Rietveld method, performed with the yttrium phase, produced abnormally high values of isotropic atomic displacement parameters, as an indication of a different site occupation from an unit cell to another. The resulting superstructure may be due to ordering between anions and vacancies, or to a shift from their ideal position.

More accurate anionic positions were expected from a neutron diffraction study where the respective neutron scattering lengths of yttrium, tantalum, oxygen and nitrogen are 7.75, 6.91, 5.805 and 9.36 fm [26]. Fig. 5, Tables 3 and 4 give details of the neutron diffraction refinement. The observations made by XRD are confirmed: a cubic fluorite structure, no superstructure peaks and high atomic displacement parameters. In addition, a wavy

background, not present in the XRD pattern, denotes a more complex structure where anions and vacancies may be ordered. Therefore, the small fluorite unit cell corresponds only to an apparent structure. Unfortunately, the sample cristallinity was not enough to get reliable results from our attempts of high resolution electron microscopy.

Acknowledgments

The authors are grateful to Françoise Bourée (Laboratoire Léon Brillouin, Saclay, France) for recording the neutron diffraction data, as well as to Thierry Roisnel (Université de Rennes 1, France) for his advices about Fullprof and WinPlotr softwares.

References

(1) Marchand, R.; Laurent, Y.; Guyader, J.; L'Haridon, P.; Verdier, P. J. Eur. Ceram. Soc. **1991**, *8*, 197.

(2) Marchand, R.; Tessier, F.; Le Sauze, A.; Diot, N. Int. J. Inorg. Mat. **2001**, *3*, 1143.

(3) Tessier, F.; Marchand, R. J. Solid State Chem. **2003**, *171*, 143.

(4) Pors, F.; Marchand, R.; Laurent, Y. J. Solid State Chem. **1993**, *107*, 39.

(5) Yoshimura, M.; Ma, J.; Kakihana, M. J. Am. Ceram. Soc. **1998**, *81*, 2721.

(6) Diot, N.; Larcher, O.; Marchand, R.; Kempf, J. Y.; Macaudière, P. J. Alloys Comp. **2001**, *323-324*, 45.

(7) Blasse, G.; Bril A. J. Lumin. **1970**, *3*, 109.

(8) Brixner, L.H.; Chen, H.Y. J. Electrochem. Soc. **1983**, *130*, 2435.

(9) Machida, M.; Murakami, S.; Kijima, T.; Matsushima, S.; Arai, M. J. Phys. Chem. B **2001**, *105*, 3289.

(10) Hitoki, G.; Takata, T.; Kondo, J.N.; Hara, M.; Kobayashi, H.; Domen, K. Chem. Commun. **2002**, *161*, 1698.

(11) Hitoki, G.; Takata, T.; Kondo, J.N.; Hara, M.; Kobayashi, H.; Domen, K. Electrochem. **2002**, *70*, 463.

(12) Hara, M.; Hitoki, G.; Takata, T.; Kondo, J.N.; Kobayashi, H.; Domen, K. Catal. Today **2003**, *78*, 555.

(13) Douy, A.; Odier, P. Mater. Res. Bull. **1989**, *24*, 1119.

(14) Boultif, A.; Louer, D. J. Appl. Cryst. **1991**, *24*, 987.

(15) Roisnel, T.; Rodriguez-Carvajal, J. *WinPLOTR: a Windows tool for powder diffraction patterns analysis*. Materials Science Forum, Proc. Seventh European Powder Diffraction Conference (EPDIC 7) **2000**, 118.

(16) Dopita, M.; Wollein, B.; Rafaja, D.; Gruner, W.; Lengauer, W. Defect and Diffusion Forum, Diffusion in Materials DIMAT-2000 **2001**, *194-199,* 1613.

(17) Markiv, V.Ya.; Belyavina, N.M.; Markiv, M.V.; Titov, Yu.A.; Sych, A.M.; Sokolov, A.N.; Kapshuk, A.A.; Slobodyanyk, M.S. J. Alloys Comp. **2002**, *346***,** 263.

(18) Titov, Yu.A.; Sych, A.M.; Sokolov, A.N.; Kapshuk, A.A.; Markiv, V.Ya.; N.M. Belyavina, N.M. J. Alloys Comp. **2000,** *311*, 252.

(19) Fonteneau, G.; L'Helgoualch, H.; Lucas, J. Mater. Res. Bull. **1977,** *12***,** 24.

(20) Marchand, R.; Pors, F.; Laurent, Y. Ann. Chim. Fr. **1991**, *16*, 553.

(21) Günther, E.; Hagenmayer, R.; Jansen, M. Z. Anorg. Allg. Chem. **2000**, *626*, 1519.

(22) Cheviré, F.; Tessier, F.; Marchand, R. Mater. Res. Bull. **2004**, *in press*.

(23) Galasso, F.S. *Structure and Properties of Inorganic Solids*, Pergamon Press, 1970.

(24) Shannon, R.D. Acta Crystallogr. **1976**, *A32*, 751.

(25) Thompson, P.; Cox, D.E.; Hastings, J.B. J. Appl. Cryst. **1987**, *20*, 79.

(26) "Neutron data booklet" (A.-J. Danoux and G. Lander, Eds), Institut Laue-Langevin, ILL Neutrons for Science, April **2002**.

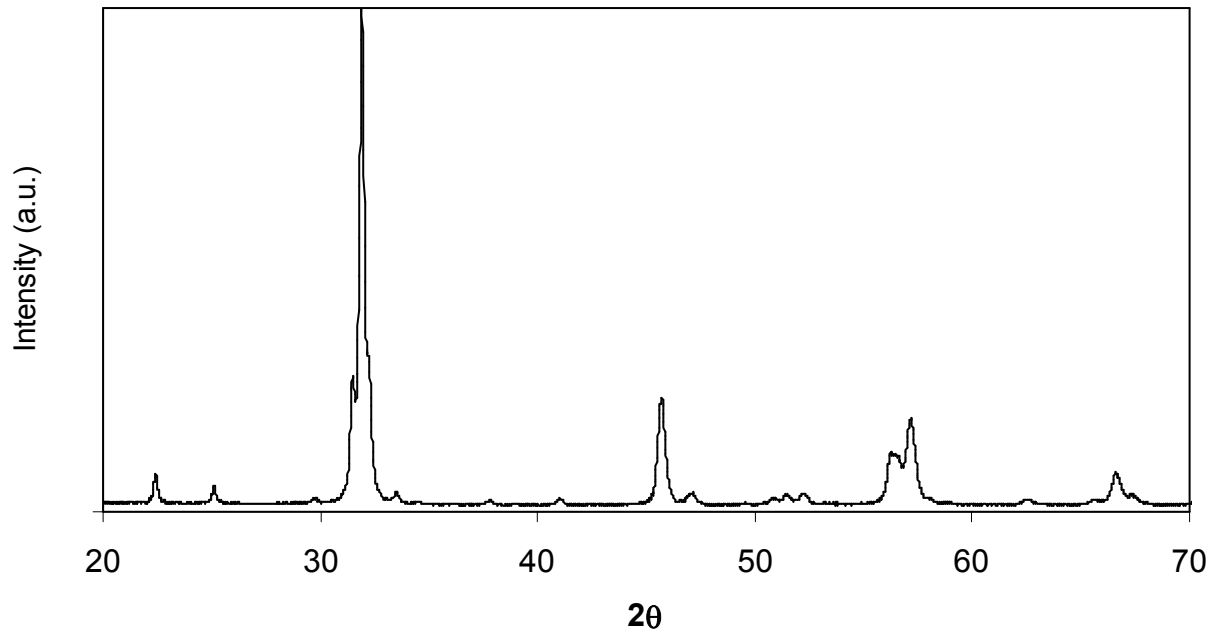

Fig. 1. XRD powder pattern of $GdTaO_2N$ after heating $GdTaO_4$ at 1000°C under ammonia flow (4x15 h cycle).

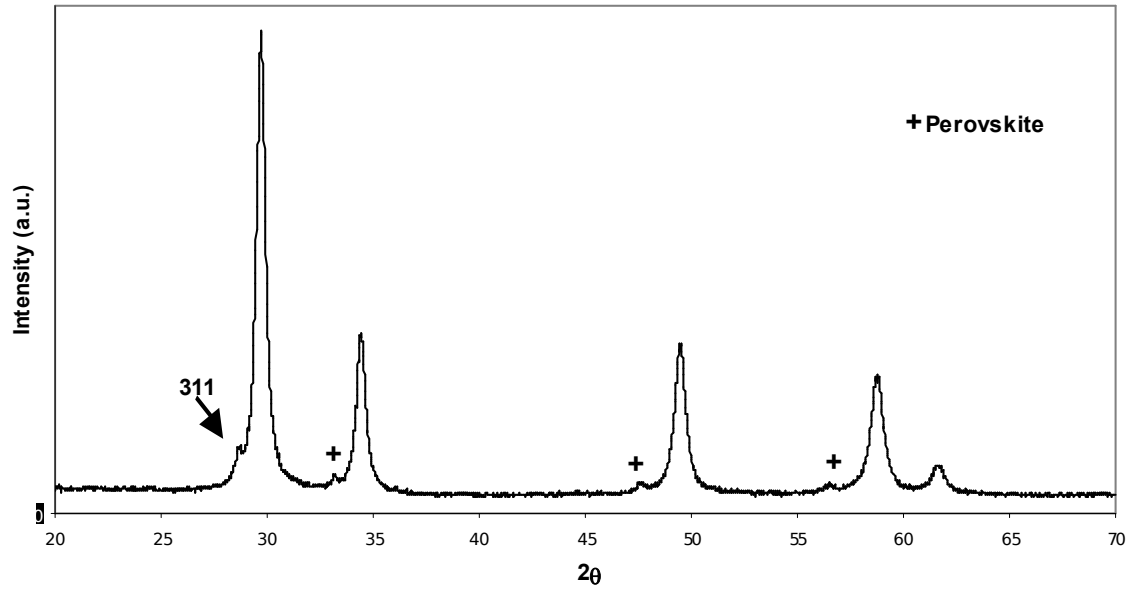

Fig. 2. XRD powder pattern of Gd-Ta-O-N after heating $GdTaO_4$ at 900°C under ammonia flow for 15 h: presence of $Gd_2Ta_2O_5N_2$ pyrochlore and $GdTaON_2$ perovskite (weak peaks with +).

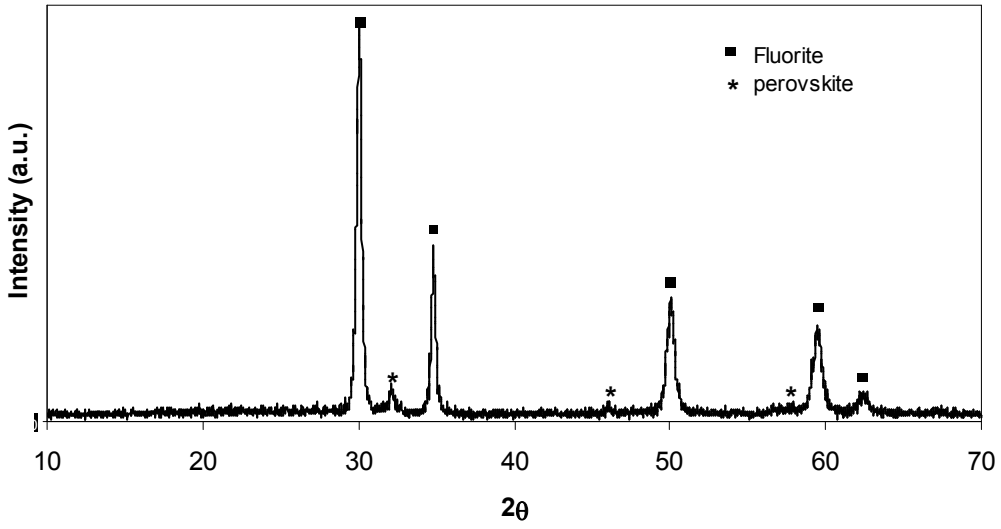

Fig. 3a. XRD powder pattern of $HoTa(O,N,\square)_4$ after ammonolysis of $HoTaO_4$ fergusonite at 950°C for 5x15 h.

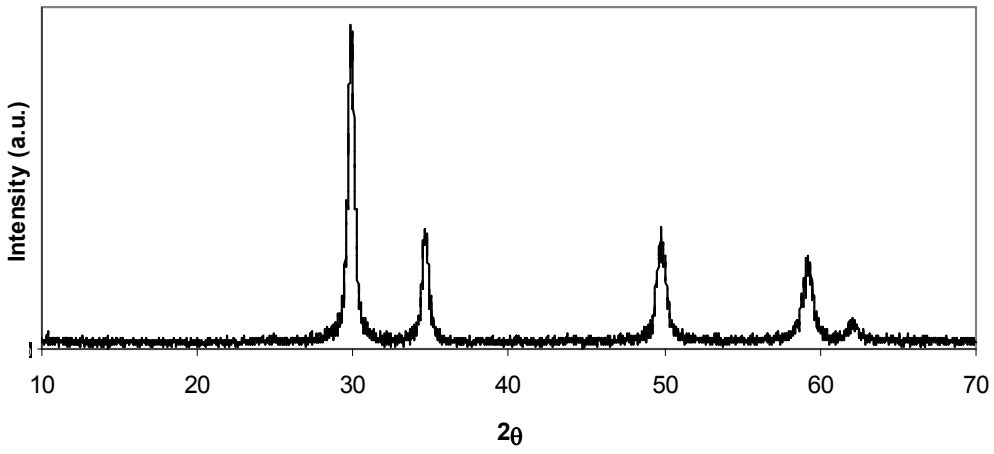

Fig. 3b. XRD powder pattern of $HoTa(O,N,\square)_4$ after ammonolysis of $HoTaO_4$ scheelite (900° C, 15 h).

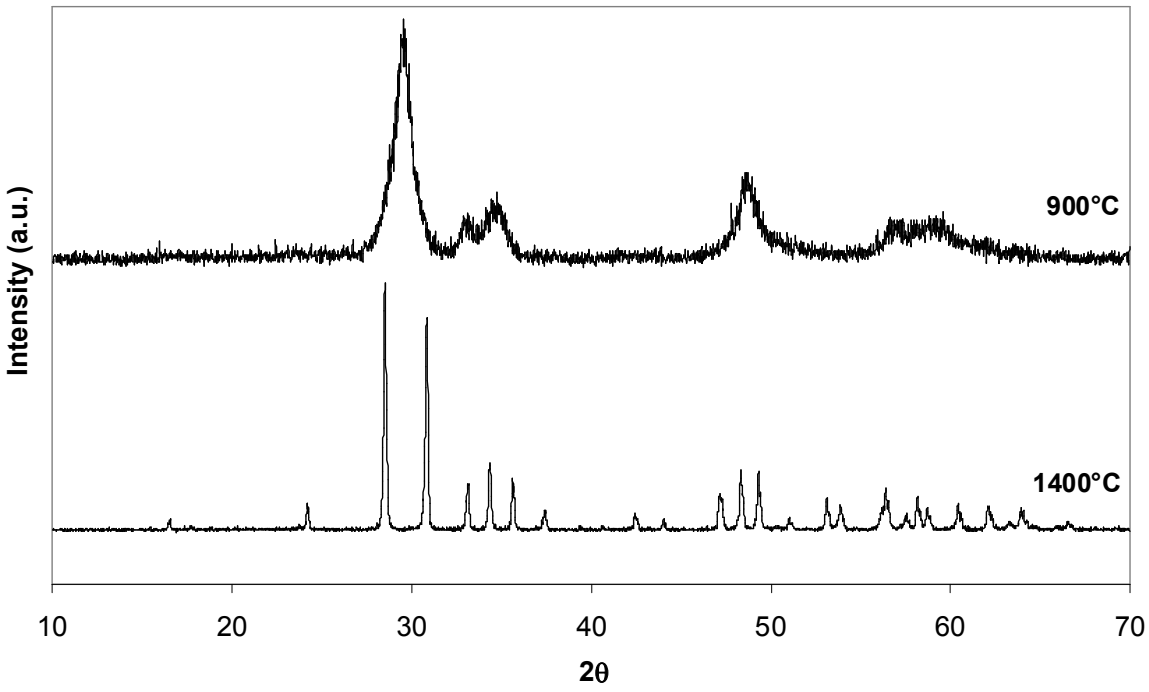

Fig. 4. Comparison between the XRD powder patterns of scheelite-type $HoTaO_4$ (citrate route, 900°C) and fergusonite-type $HoTaO_4$ (ceramic route, 1400°C).

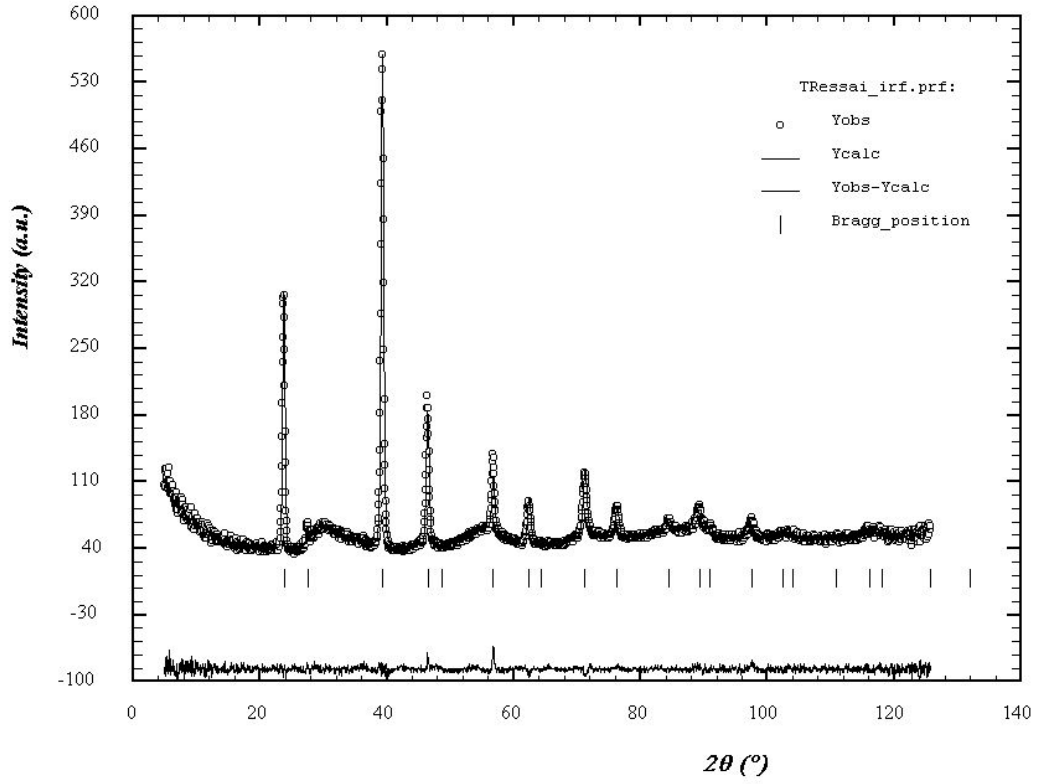

Fig. 5. Neutron diffraction powder pattern of the $YTa(O,N,\square)_4$ fluorite phase (N wt.% = 4.66).

Table 1. Competition between pyrochlore ($R_2Ta_2O_5N_2$) and perovskite ($RTaON_2$) structures within the R-Ta-O-N systems. (parameters after [4, 20], except for *: this study). From Dy toYb, pyrochlore and defect-fluorite solid solutions parameters, determined in this study, are related by a factor 2.

R	La	Nd	Sm	Gd	Dy	Ho	Y	Er	Yb
Pyrochlore unit cell (Å)	-	10.56	10.501	10.44 10.42(1) *	10.34	10.327	10.301	10.282	10.235
Perovskite unit cell (Å)	a = 8.0922(31) b = 8.0603(2) c = 5.7118(2) β = 134.815(1)°	a = 5.671 b = 5.671 c = 8.080	a = 5.590 b = 5.705 c = 7.974	a = 5.552(3) * b = 5.690(2) c = 7.923(3)	-	-	-	-	-

Table 2. $RTa(O, N, \square)_4$ fluorite-type solid solutions: nitridation and unit cell parameters.

R	Thermal ammonolysis conditions	N wt.%	Experimental formulation	Cubic unit cell parameter (Å)
Ho	15h, 900°C	2.08	$HoTaO_{3.10}N_{0.60}\square_{0.30}$	5.170(2)
	6 x 15h, 950°C	3.24	$HoTaO_{2.61}N_{0.93}\square_{0.46}$	5.1572(6)
Y	15h, 900°C	3.56	$YTaO_{2.76}N_{0.83}\square_{0.41}$	5.1675(5)
	6 x 15h, 950°C	4.66	$YTaO_{2.39}N_{1.08}\square_{0.53}$	5.1555(2)
Er	15h, 900°C	2.97	$ErTaO_{2.83}N_{0.78}\square_{0.39}$	5.156(2)
	6 x 15h, 950°C	3.19	$ErTaO_{2.62}N_{0.92}\square_{0.46}$	5.1507(7)

Table 3. Details of Rietveld refinement for the $YTa(O,N,\square)_4$ fluorite phase (N wt.% = 4.66).

.

a (Å)	5.15268 (6)
V (Å^3)	136.8
Space group	$Fm\bar{3}m$
Z	4
λ (Å)	1.2251
No. of reflections	22
Profile function	TCH [25]
R_p	28.6
R_{wp}	15.2
R_{exp}	12.91
χ^2	1.39

Table 4. Fractional atomic coordinates and isotropic displacement parameters for the $YTa(O,N,\square)_4$ fluorite phase (N wt.% = 4.66).

Atom	Position	x	y	z	Occupation	Biso ($Å^2$)
Y	4a	0	0	0	0.5	2.11
Ta	4a	0	0	0	0.5	2.11
O	8c	1/4	1/4	1/4	0.53	6.95
N	8c	1/4	1/4	1/4	0.31	6.95